Comparison of spray quality for two different flow configurations: Central liquid jet versus annular liquid sheet

Simon Wachter*[1], Tobias Jakobs[1], Thomas Kolb[1,2]
[1]Karlsruhe Institute of Technology, Institute for Technical Chemistry, 76344 Eggenstein-Leopoldshafen, Germany
[2]Karlsruhe Institute of Technology, Engler-Bunte-Institute, 76131 Karlsruhe, Germany
*Corresponding author: simon.wachter@kit.edu

Abstract
The research work of the present study is focused on the detailed comparison of two external mixing twin fluid nozzle concepts: (i) a central liquid jet with annular gas stream, (ii) an annular liquid sheet with central gas jet. Both nozzle types are applied in high pressure entrained flow gasifiers (EFG), where atomization is characterized by low Gas-to-liquid ratio (GLR) and high fuel viscosity. In order to compare spray formation as well as atomization efficiency in terms of Sauter mean diameter, a nozzle with equal orifice area of the gas and liquid exit is investigated. The nozzle enables equal atomization conditions concerning GLR, liquid mass flow, velocity of liquid and gas, as well as momentum flow ratio for both nozzle configurations. 4 Newtonian liquids: water and three glycerol/water mixtures with viscosity of 1mPas, 50mPas, 100mPas and 200mPas are used for the experiments in both nozzle configurations at various GLR. For spray analysis, a high speed camera, a shadowgraphy system as well as a phase-doppler analyzer are applied. The use of three different measuring techniques allows for characterization of primary breakup as well as local drop size distribution. With the high speed camera the breakup regime morphology is detected and classified for both operating configurations. Radial measurements of the local Sauter mean diameter are conducted with the phase-doppler analyzer. Furthermore, the spray angle is detected and the integral Sauter mean diameters for all operating conditions is compared for both nozzle configurations to evaluate atomization efficiency.

Keywords
External mixing twin-fluid atomization; comparison jet vs sheet nozzle; breakup morphology; drop size distribution

Introduction
High pressure entrained flow gasification (EFG) is a key technology to enable a future carbon neutral circular economy, by closing the carbon cycle through conversion of biomass and waste based feedstocks to syngas ($CO + H_2$). EFG typically uses oxygen as gasification agent, which also serves as atomization agent, in consequence Gas-to-Liquid ratios (GLR) < 1 are applied [1]. Commonly external mixing twin-fluid atomizers are used, due to their advantages concerning abrasion and clogging. Experimental and theoretical investigations regarding external mixing twin-fluid atomization, can be divided into two different configurations. The first configuration provides the liquid via a central tube surrounded by a concentric high-velocity annular gas sheet. Detailed investigations on liquid jet breakup morphology of this configuration using water were performed by Faragò, Chigier [2] and expanded by Lasheras and Hopfinger [3]. The breakup was classified into spray regimes showing with increasing Weber number at constant liquid Reynolds number a transition from the Rayleigh type to Membrane and fiber type breakup with the submodes pulsating and superpulsating. Studies on drop size resulting from this configuration applying Newtonian viscous liquids in a viscosity range of η_{liq} = 1 – 100mPas and GLR = 1 - 12 were conducted by Lorenzetto [4], Jasuja [5], Rizk [6] and Walzel [7]. For GLR < 1 and various liquid viscosities, Sänger [8] reported integral drop sizes and detected moreover two different new primary instability modes influencing the resulting drop size. The second nozzle configuration provides the liquid through an annular gap forming a liquid sheet with a high-speed gas jet emerging from a central tube. Applying this configuration, Leboucher et al. [9] and Zhao et al. [10] reported morphological studies on liquid sheet disintegration for water, using different diagrams for interpretation of their results. The authors classified the breakup regimes bubble type, Christmas tree and fibre-type breakup with increasing Weber number depending additionally on the geometry of the nozzle orifice. Experimental work including drop size measurements of water were conducted by Li et al. [11], applying gas velocities v_{gas} > 180ms^{-1} and Leboucher et al. [9], using different system pressures and swirl configurations.

Summing up, for atomization using external mixing twin-fluid atomizers with liquid supplied through an annular gap most experimental investigations were performed using low viscous liquids and GLR > 1, which is not relevant for EFG operation. Additionally, previous studies do not allow for a comparison of primary breakup and drop size between the two nozzle configurations, due to different measurement and operating conditions or nozzle designs. In this context, the present research applies both nozzle configurations, with equal orifice areas leading to constant

operating conditions in terms of GLR, $\dot{m}_{liq}$, v_{gas} and momentum flux ratio in both operating modes. Measurements were conducted for liquids with different dynamic viscosities and GLRs relevant for EFG, using a high-speed camera for visualization of primary jet breakup, a shadowsizer for validation purpose and a phase doppler analyzer for local drop size measurements with high radial resolution.

Experimental setup

The experimental setup used in the present work consists of an atmospheric spray test rig (ATMO), a phase doppler analyzer (PDA), a shadowgraphy system and a high-speed camera. For spray generation an external mixing twin-fluid atomizer was applied for atomization of water and several glycerol/water-mixtures.

The spray test rig ATMO is schematically shown in Figure 1. The atomizer is mounted on the twin-fluid lance with liquid supply from a tempered tank. The liquid is delivered by an eccentric screw pump (mass flow range 5 – 40kgh^{-1}) and controlled by a Coriolis mass flow meter. Liquid viscosity η_{liq} can be applied in a range of 1 to 1000mPas. Compressed air in the range of 1-20kgh^{-1} is fed to the top of the lance, the air mass flow $\dot{m}_{gas}$ is controlled by a mass flow controller. A honeycomb structure at the inlet of the collection tank serves as flow conditioner, a suction of exhaust air prevents recirculation of small droplets. Fully optical access to the spray enables the use of different laser based measurement systems as well as a high-speed camera.

Experiments were carried out using the external mixing twin-fluid atomizer shown in Figure 1, which can be operated in both configurations discussed above, due to the equal area of the inner and outer orifice. For the discussion of the results, the following nomenclature is used:

(i): Liquid in central tube, gas flow through concentric annular gap.

(ii): Gas in central tube, liquid flow through concentric annular gap.

The central tube has a diameter of D_{inner} = 5.4mm and is surrounded by an annular gap with a width of 1.09mm, which leads to identical orifice areas. For minimization of the area between inner and outer orifice, the wall thickness b was set to 0.1mm. In addition, to reduce the influence of flow induced disturbances, as well as to enable comparability towards experimental results of Faragò, Chigier [12] and Zhao et al [10], the nozzle has parallel flow channels.

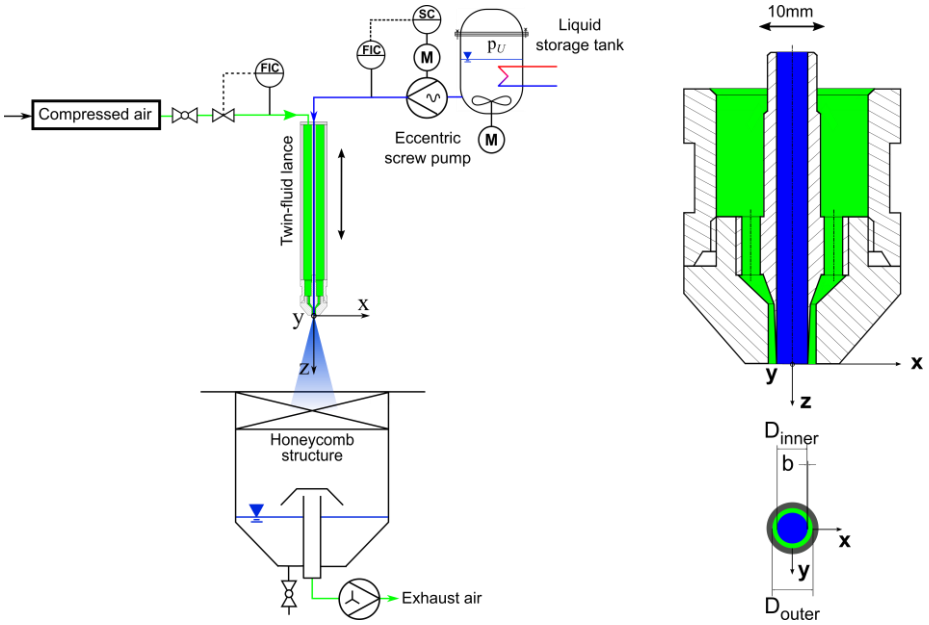

Figure 1. Schematic of the experimental setup applying nozzle configuration (i) – atmospheric spray test rig (ATMO) (left); Schematic of the nozzle geometry and orifice view applying nozzle configuration (i) (right)

Table 1. Physical properties of all used liquids at 20°C and 1atm

	η_{liq} [mPas]	σ [kgs^{-2}]	ρ_{liq} [kgm^{-3}]
water	1	0.0728	998
glycerol/water (78.5 wt.%)	50	0.0656	1204
glycerol/water (84.5 wt.%)	100	0.0649	1220
glycerol/water (89.5 wt.%)	200	0.0642	1233

For the investigation of liquid viscosity η_{liq} on the primary spray breakup and drop size, water and three different glycerol/water – mixtures were used. Surface tension and density of the four liquids applied are almost constant (see Table 1). Liquid viscosity was quantified applying a Physica MCR 101 rheometer from Anton Paar with Searle

type measuring system [13]. Surface tension and density were measured with an EasyDyne tensiometer from Krüss using the Du Noüy ring method [14] and the weighing method, respectively. Mass ratio, viscosity, surface tension and density for all liquids are shown for 20°C and 1atm in Table 1.

A Photron SA4 high speed camera for qualitative investigation of the primary breakup process was employed close to the nozzle orifice. The camera features a frame rate of 3.6kHz at a resolution of 1024 x 1024 pixel and frame rates up to 500kHz at reduced resolution. The images were captured by backlight illumination with a special lighting setup, including an array of 9 high-power light-emitting diodes (LED) with total luminous flux of 9 x 4500lm. To guarantee for a qualitative investigation of the liquid disintegration process a set of 1000 high-speed images was recorded at every operating condition as well as a background reference image without liquid flow.
To measure droplet size with high spatial and temporal resolution within the spray cone a Fiber PDA by Dantec Dynamics was used. For data collection the PDA was operated in forward scattering arrangement, refraction mode (1st – order) using the asymmetric Mask B. To guarantee for the detection of large droplets as expected by the atomization of high viscous liquids and avoid sizing errors due to the Gaussian beam effect according to Araneo [15] the PDA was set as shown in Table 2. With this optical configuration, the PDA system allows for detection of droplets with minimum size of 1µm and maximum size of 1307µm in case of water and 1330µm in case of the glycerol/water mixtures, related to the refractive index of the liquid [16]. To improve the PDA settings a sensitivity study as described in [17] was performed. For validation purpose towards sphericity of the droplets a shadowsizer was employed, recording 1000 images for each operational condition.

Table 2. Settings of the Fiber PDA evaluated by the sensitivity analysis

Parameters	Values	Unit	Parameters	Values	Unit
Transmitter focal length	1000	mm	Laser wavelength	514.5	nm
Receiver focal length	1000	mm	Laser power (Transmitter exit)	25	mW
Beam expander ratio	1	-	Off-axis angle	70	°
Receiver slit width (physical)	200	µm	Frequency shift	40	MHz

To enable drop size measurements at several horizontal positions within the spray cone, receiver and transmitter were mounted on a traverse, which guarantees for spatially reproducible operation < 0.1mm. Data were obtained by moving the detection volume relatively to the nozzle position. The measurements were taken at several radial (traverse along x – axis) positions with a radial increment of Δx = 2 - 4mm depending on the operating conditions. According to the orientation of the coordinate system as indicated in Figure 1 and the alignment of the fringes of the laser beam couple (λ_L = 514.5nm - green), axial- v_z droplet velocity component could be measured. To ensure a reliable database for every radial position during PDA measurements as termination criterion sample size and measurement time were set to 50000 droplets or 60 seconds, respectively. For every radial position, at least 15000 droplets were detected. The raw data from the manufacturer software were used to compute arithmetic means, statistical data as well as additional information using the toolbox *SprayCAT*, according to Sänger [8]. Further Information concerning computation of global size distribution and drop size moments can be obtained from DIN SPEC 91325 as well as from Albrecht [16]. All PDA measurements were conducted at an axial distance of z = 200mm from the nozzle orifice and repeated at least 3 times. For each operating condition and nozzle configuration, rotational symmetry of the spray cone was proven, taking a full radial profile in a first set of experiments. After rotational symmetry was proven, the following repetition measurements were performed taking half profiles from the spray edge to the centre at x = 0mm. The results of those set of experiments were afterwards mirrored to get full profiles. Therefore all radial Sauter diameter distributions are shown as mirrored profiles at x = 0mm.

Results and discussion

In order to investigate the influence of the nozzle configuration on spray quality for the external mixing twin-fluid atomizer described above, experiments were conducted at operating conditions presented in Table 3. For all experiments, pressurized air at 20°C was used as atomization agent.

Table 3. Operating conditions of the experiments for both nozzle configurations

η_{liq} [mPas]	$\dot{m}_{gas}$ [kgh^{-1}]	$\dot{m}_{liq}$ [kgh^{-1}]	v_{gas} [ms^{-1}]	GLR [-]
1/50/100/200	3/6/9/12/15	30	30/60/90/120/150	0.1/0.2/0.3/0.4/0.5

Influence of the nozzle configuration on spray quality

For quantitative comparison of the two nozzle configurations as well as for the description of the influence of liquid viscosity and GLR on Sauter mean diameter, radial measurements were performed (see Figure 2). For reasons of improved clarity, only data for GLR = 0.3 and 0.5 are shown as radial profiles. It has to be mentioned, that Figure 2 shows local values for η_{liq} = 1mPas (x ≤ 0mm) and η_{liq} = 50mPas (x ≥ 0mm).

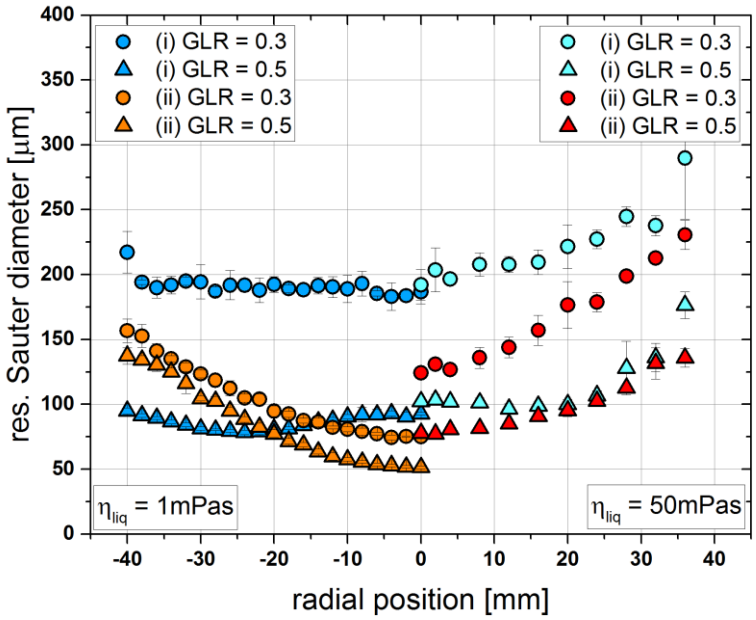

Figure 2. Radial measurements (z = 200mm) of resulting Sauter Diameter using both nozzle configurations (i) at GLR = 0.3 and 0.5 – liquid viscosity η_{liq} = 1mPas (left), liquid viscosity η_{liq} = 50mPas (right)

Comparing the radial shape of droplet size distributions, nozzle configuration (i) shows an almost constant Sauter mean diameter over the radial profile for low liquid viscosity, whereas at higher liquid viscosity a v-shaped profile is detected, with higher droplet size at the outer boundary. For nozzle configuration (ii) a v-shaped profile was detected for both viscosities and GLR with a minimum Sauter mean diameter on the spray axis.

As expected, with increasing GLR, for both nozzle configurations and both viscosities, a decreasing Sauter mean diameter was measured. With increasing liquid viscosity, Sauter mean diameters for all operating conditions are increased. For low liquid viscosity applying nozzle configuration (i) the decrease of droplet size is significantly higher, compared to nozzle configuration (ii), i.e. nozzle configuration (ii) is less sensitive to GLR. Comparing the nozzle configurations applying higher liquid viscosity, an increasing GLR leads to significant lower Sauter mean diameters for both nozzle configurations.

In order to compare all experiments with the two different nozzle configurations (i) and (ii) regarding spray quality, the mass weighted integral Sauter diameter (ID_{32}) was calculated as proposed by Sänger [8]; data are plotted in Figure 3. For all experiments a decrease in ID_{32} with increasing GLR is observed. With increasing liquid viscosity, the ID_{32} value increases significantly for both nozzle configurations for GLR < 0.4. For GLR ≥ 0.4 and different viscosities the deviation in the ID_{32} value is marginal. Comparing both nozzle configurations, the ID_{32} value is decreasing with a larger gradient using nozzle configuration (i). In contrast to this, the ID_{32} value for nozzle configuration (ii) is remarkably lower at GLR < 0.4 compared to configuration (i). At GLR = 0.5, it is worth mentioning, that nozzle configuration (i) has already a lower ID_{32} than configuration (ii). This is caused by slow droplets at the edge of the spray cone, resulting from the disintegrated sheet of nozzle configuration (ii), moving in a region with small aerodynamic forces.

For additional comparison, spray angle was estimated based on 1000 high speed camera images at each operating condition was done, applying the method for spray angle determination according to Sänger [8]. Exemplarily and for improved clarity only two viscosities at different GLR are shown in Figure 4.

Applying low viscosity for nozzle configuration (i) a strictly monotonic decrease of spray angle with increasing GLR is observed, whereas configuration (ii) shows nearly constant spray angle values for all GLR. With increased viscosity applying nozzle configuration (i), same dependence on GLR is detected for larger spray angles. For nozzle

configuration (ii) and increased viscosity, lower spray angle values are detected, showing also constant values for GLR variation, except for GLR = 0.5.

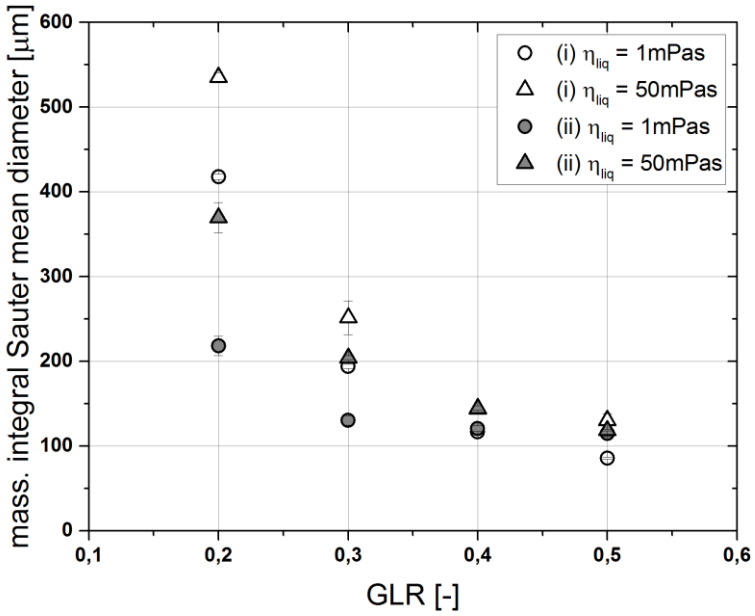

Figure 3. Influence of liquid viscosity and GLR on mass weighted integral Sauter diameter comparing nozzle configurations at z = 200mm

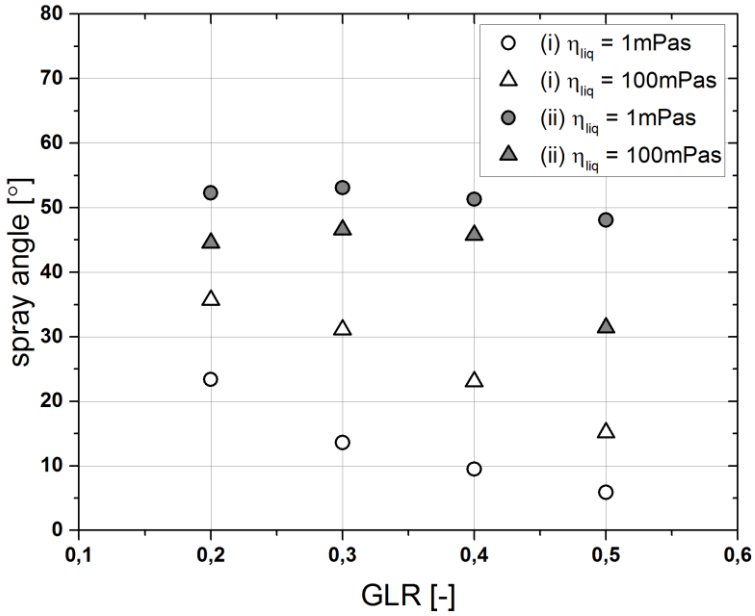

Figure 4. Influence of liquid viscosity and GLR on spray angle, measured by high speed camera images, comparing nozzle configurations

Observed primary breakup for different nozzle configurations, liquid viscosity and GLR

For visualization of the spray, high speed camera images of primary jet breakup applying nozzle configuration (i) at different GLR and liquid viscosity are shown in Figure 5. The images are framed in different colours indicating various spray quality.

Increasing viscosity at low GLR (blue) leads to the formation of membranes at the spray centre, which result in large elongated ligaments after disintegration of the membrane; this is caused by the damping effects of increased liquid viscosity. For viscosities up to 100mPas and increasing GLR ≥ 0.3 (green) the jet disintegration occurs close to the nozzle orifice due to the fast surrounding gas flow, producing a homogeneous spray according to Figure 2(left) with a decreasing spray angle as shown in Figure 4. Applying liquid viscosities up to 200mPas and GLR ≥ 0.3 (red) the

primary jet is disintegrated into partly radial elongated ligaments, which move out of the spray centre, leading to larger droplets at the spray outer boundary and an increased spray angle as also shown in Figure 4.

According to the regime classification of Lasheras et al. [3] and Zhao et al. [10], for low gas velocities at the nozzle orifice (GLR = 0.1), the liquid jet is slightly elongated and reduced in diameter due to aerodynamic forces, which leads to Rayleigh type breakup. For increasing gas velocity (GLR = 0.2), and with increasing liquid viscosity even more visible, the membrane type breakup disintegrates the liquid jet, producing long ligaments and large membranes. Between GLR = 0.3 and GLR = 0.4 the fiber type pulsating mode occurs, which atomizes the liquid jet directly at the nozzle orifice into small fibres and droplets. Changes in local droplet density mark the transition region between the submodes pulsating and superpulsating at higher gas velocities (GLR = 0.5).

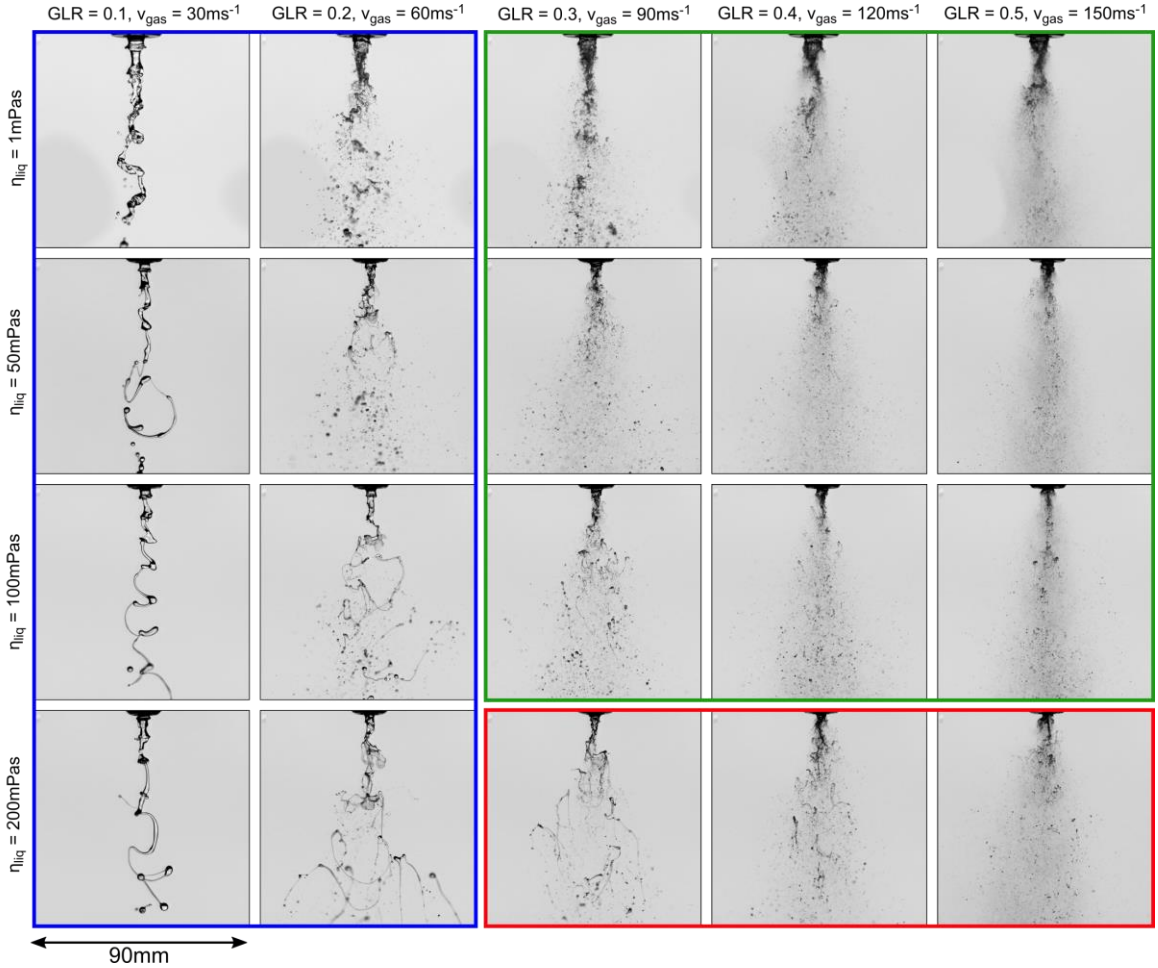

Figure 5. High-speed camera images of the primary liquid disintegration process using nozzle configuration (i), different liquid viscosities and GLR (i.e. v_{gas})

The corresponding high-speed camera images for nozzle configuration (ii) are shown in Figure 6. For increasing viscosity and low GLR (blue), a compact sheet exits the nozzle orifice and is disintegrated into large droplets or ligaments, due to the low gas velocity. With increasing GLR and for all viscosities (red), the liquid sheet disintegrates closer to the nozzle orifice into droplets. Due to the faster gas jet in the spray centre, the resulting droplets are smaller, whereas ligaments moving out of the spray centre are not further disintegrated, due to the slow gas flow in this region. For further increasing GLR and all viscosities (green), the drop size in the spray centre is decreasing, which leads to regions with varying droplet number density. The further decrease in drop size at the edge of the spray cone is marginal, due to the low gas velocity in this area. A nearly constant spray angle is detected, which is independent of gas velocity, due to the steady disintegration of the liquid sheet at the nozzle orifice (see Figure 4).

For GLR > 0.2, the classification diagram of Zhao et al. [10] predicts the Christmas tree breakup with characteristic horizontal compact liquid fragments for nozzle configuration (ii); this effect cannot be seen in the high speed images of Figure 6. However changes of the morphology of jet disintegration for higher gas velocities (GLR ≥ 0.3), like small fibres near the nozzle orifice and droplet density variations in the spray centre similar to a fibre type breakup in pulsating or superpulsating submode according to Lasheras et al. [2,3] can be observed.

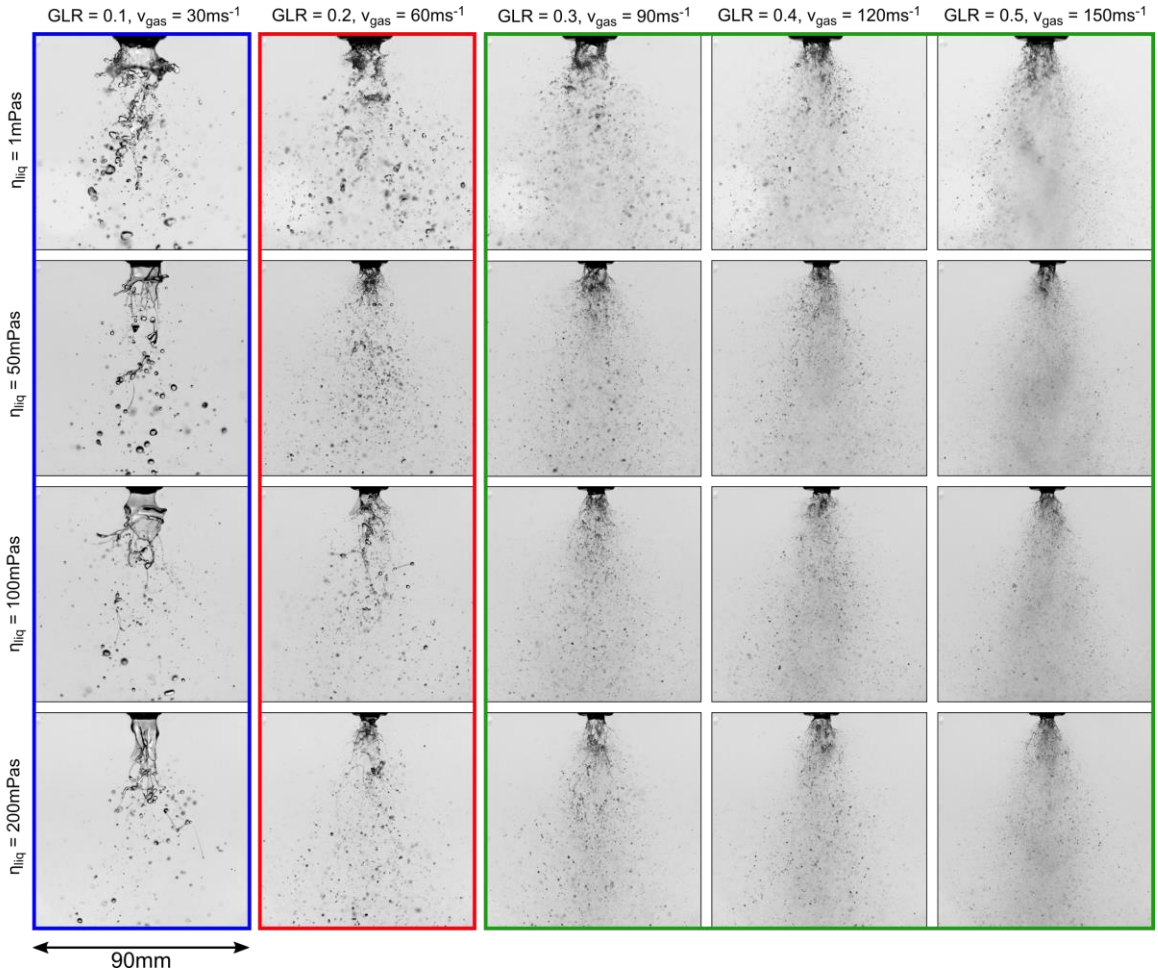

Figure 6. High-speed camera images of the primary liquid disintegration process using nozzle configuration (ii), different liquid viscosities and GLR (i.e. v_{gas})

Conclusions

In the present study two different external mixing twin-fluid nozzle configurations (central liquid jet (i) and liquid sheet (ii)) with equal orifice areas for liquid and gas are compared. This nozzle geometry allows for constant operating conditions (GLR, $\dot{m}_{liq}$, v_{gas} and momentum flux ratio) for both configurations. Liquid viscosity and GLR (i.e. gas velocity) were varied and local Sauter mean diameter, mass weighted integral Sauter diameter, as well as spray angle and primary breakup morphology were detected.

In general, nozzle configuration (i) achieves better spray quality (i.e. lower integral Sauter mean diameter) for increased GLR and low liquid viscosity. Applying nozzle configuration (ii) improved spray quality for low GLR and higher liquid viscosities is observed. As a drawback larger droplets at the boundary of the spray occur. Furthermore nozzle configuration (ii) leads to increased and constant spray angles, compared to configuration (i). Comparing quantitative and qualitative findings, the following detailed conclusions can be drawn:

(1) For nozzle configuration (i), a nearly constant radial Sauter mean diameter profile is observed for low liquid viscosity and both GLRs. For all operating conditions applying configuration (ii) larger droplets at the boundary of the spray cone are detected.

(2) With higher liquid viscosity for both nozzle configurations, Sauter mean diameters are increased, caused by the damping effects of the liquid. The sensitivity of Sauter mean diameter on GLR is higher applying nozzle configuration (i) than for nozzle configuration (ii).

(3) The measured spray angle stays nearly constant for nozzle configuration (ii) over the range of investigated GLR. With increasing liquid viscosity, the spray angle is slightly decreased. Applying configuration (i), the spray angle decreases with increasing GLR for both viscosities. With higher liquid viscosity, the spray angle is increased, due to the radially elongated ligaments produced.

Acknowledgements

The authors gratefully acknowledge the financial support by the Helmholtz Association of German Research Centers (HGF), within the research field Energy, Material and Resources, Topic 4 Gasification (34.14.02). The present work contributes to the Helmholtz Virtual Institute for Gasification Technology–HVIGasTech (VH-VI-429).

Nomenclature

b	wall thickness [mm]	GLR	Gas-to-liquid ratio [-]	v_{gas}	orifice gas velocity [ms^{-1}]
D_{inner}	inner diameter [mm]	ID_{32}	integral Sauter diam. [µm]	x, y, z	coordinate axis [mm]
D_{outer}	outer diameter [mm]	$\dot{m}_{gas}$	gas mass flow [kgh^{-1}]	η_{liq}	dy. liquid viscosity [mPas]
D_{32}	Sauter diameter [µm]	$\dot{m}_{liq}$	liquid mass flow [kgh^{-1}]	ρ_{liq}	liquid density [kgm^{-3}]
f	data rate [s^{-1}]	r	length [mm]	σ	surface tension [Nm^{-1}]

References

[1] Jakobs T., Djordjevic N., Fleck S., Mancini M., Weber R., and Kolb T., 2012,“Gasification of high viscous slurry R&D on atomization and numerical simulation,” Applied Energy, **93**, pp. 449–456.

[2] Chigier N., and Faragó Z., 1992,“Morphological Classification of Disintegration of Round Liquid Jets in a Coaxial Air Stream,” Atomization and Sprays, **2**(2), pp. 137–153.

[3] Lasheras J. C., Villermaux E., and Hopfinger E. J., 1998,“Break-up and atomization of a round water jet by high-speed annular air jet,” J. Fluid Mech., **357**, 351 379.

[4] Lorenzetto G. E., and Lefebvre A. H.,“Measurements of Drop Size on a Plain-Jet Airblast Atomizer,” AIAA Journal, **15**(7), pp. 1006–1010.

[5] Jasuja A. K., 1982,“Plain-Jet Airblast Atomization of Alternative Liquid Petroleum Fuels Under High Ambient Air Pressure Conditions,” The american society of mechanical engineers(3).

[6] Rizk N.K., and Lefebvre A.H., 1984,“Spray characteristics of plain-jet airblast atomizers,” ASME, **634**(106).

[7] Schmidt P., and Walzel P., 1980,“Zerstäuben von Flüssigkeiten,” Chemie Ingenieur Technik, **52**(4), pp. 304–311.

[8] Alexander Daniel Sänger, 2018. *Zerstäubung hochviskoser Fluide bei variierendem Systemdruck - Grundlagenforschung zur Hochdruck-Flugstromvergasung*.

[9] Leboucher N., Roger F., and Carreau J.-L., 2012,“Characteristics of the spray produced by the atomization of an annular liquid sheet assisted by an inner gas jet,” Atomization and Spray, **22**(6), pp. 515–542.

[10] Zhao H., Xu J.-L., Wu J.-H., Li W.-F., and Liu H.-F., 2015,“Breakup morphology of annular liquid sheet with an inner round air stream,” Chemical Engineering Science, **137**, pp. 412–422.

[11] Li X., and Shen J., 1999,“Experimental Study of Sprays from Annular Liquid Jet Breakup,” Journal of Propulsion and Power, **15**(1), pp. 103–110.

[12] Chigier N. A., and Farago Z., 1992,“Morphological classification of disintegration of round liquid jets in a coaxial air stream,” Atomization and Sprays, pp. 137–153.

[13] Searle G.F.C.,“Simple Viscometer for Very Viscous Liquids,” Proceedings of the Cambridge Philosophical Society, Mathematical and physical sciences, **1912**.

[14] du Nouy, P. L., 1925,“An Interfacial Tensiometer for Universal use,” The Journal of General Physiology, **7**(5), pp. 625–631.

[15] Araneo L., Damaschke N., and Tropea C., 2002,“Measurement and Prediction of the Gaussian Beam Effect in the PDA,” Springer, pp. 189–208.

[16] Albrecht H.-E., 2003. *Laser doppler and phase doppler measurement techniques*, Springer, Berlin, New York.

[17] Kapulla R., and Najera S. B., 2006,“Operation conditions of a phase Doppler anemometer: droplet size measurements with laser beam power, photomultiplier voltage, signal gain and signal-to-noise ratio as parameters,” Meas. Sci. Technol., **17**(1), pp. 221–227.

[18] Hede P. D., Bach P., and Jensen A. D., 2008,“Two-fluid spray atomization and pneumatic nozzles for fluid bed coating / agglomeration purposes: a review,” Chemical Engineering Science, **63**, pp. 3821–3842.